

Communication

1,3-Diphenyl-5-(9-phenanthryl)-2-pyrazoline (DPPhP): An Excellent Hole-Transport Material for Use in Organic Light-Emitting Diodes

MA, Chang-Qi^a(马昌期) ZHANG, Lian-Qi^a(张联齐) ZHOU, Jia-Hong^a(周家宏)
WANG, Xue-Song^{*a}(王雪松) ZHANG, Bao-Wen^{*a}(张宝文) CAO, Yi^a(曹怡)
BUGNON, P.^b SCHAER, M.^b NÜESCH, F.^b ZHANG, De-Qiang^c(张德强) QIU, Yong^c(邱勇)

^a Technical Institute of Physics and Chemistry, Chinese Academy of Sciences, Beijing 100101, China

^b Département de Physique, Ecole Polytechnique Fédérale de Lausanne, EPFL, Lausanne, Switzerland

^c Department of Chemistry, Tsinghua University, Beijing 100084, China

An excellent hole-transport material, 1,3-diphenyl-5-(9-phenanthryl)-2-pyrazoline (DPPhP) for OLEDs was studied. This compound not only offers high glass transition temperature ($T_g = 96\text{ }^\circ\text{C}$), good film forming ability, and high HOMO energy level, but also displays excellent hole-transport property. The electroluminescent device with a simple structure of ITO/DPPhP (60 nm)/AlQ (60 nm)/LiF (0.8 nm)/Al shows an external quantum efficiency as high as 1.6%.

Keywords pyrazoline, hole-transport, thermal stability, film forming ability, external quantum efficiency

Organic light-emitting diodes (OLEDs) using small organic molecules have received considerable interest after the initial work by Tang *et al.*¹ in 1987, for the potential of using these devices as low-cost alternative in lighting, back light and flat panel displays. Much progress has been made recently in improving the efficiencies of the electroluminescent (EL) devices by using multilayered structures,² doped emitting layers,³ novel materials⁴ and efficient injection contacts.⁵ One key to increase the efficiency of an OLED device is to balance the charge carrier transport by adding a hole-transport layer and an electron-transport layer to the diode structure. The hole-transport layer in OLEDs provides efficient hole injection from the anode into the emitting layer and blocks electrons within this layer, in order to maximize the recombination proba-

bility of the injected carriers at the interface formed by the organic materials. Recently a lot of hole-transport materials (HTM) with high glass transition temperatures (T_g), predominantly based on the triarylamine functionality, including starburst amines,⁶ spiro-linked amines,⁷ and those with rigid groups⁸ have been investigated. Among these materials, *N, N'*-di-1-naphthyl-*N, N'*-diphenyl-1, 1'-biphenyl-4,4'-diamine (α -NPD)⁹ is the most prevalent and has a T_g of 98 $^\circ\text{C}$. The high T_g prevents the HTM from recrystallization and resultantly improves the stability of OLEDs. 1,3,5-Triaryl-2-pyrazoline compounds have been used as hole-transport materials in OLEDs for their good hole-transporting ability, while most of them have low T_g and show poor thermal stability.¹⁰ In this paper, we report a novel hole-transporting material 1,3-diphenyl-5-(9-phenanthryl)-2-pyrazoline (DPPhP) with T_g as high as 96 $^\circ\text{C}$ for OLEDs. This compound not only offers good film forming ability, high HOMO energy level, but also displays excellent hole-transport property. Fig. 1 shows the molecular structures of DPPhP, α -NPD and tris(8-hydroxyquinolino)aluminum (AlQ). DPPhP was prepared in about 72% yield according to the reported methods,¹¹ and its structure was confirmed by ¹H NMR and mass spectra.¹² Fig. 2 shows the DSC thermograms of DPPhP. When the crystalline sample of DPPhP was

* E-mail: g203@ipc.ac.cn

Received March 15, 2002, revised August 5, 2002; accepted August 7, 2002.

Project supported by the National Natural Science Foundation of China (Nos. 29971031 and 20073050).

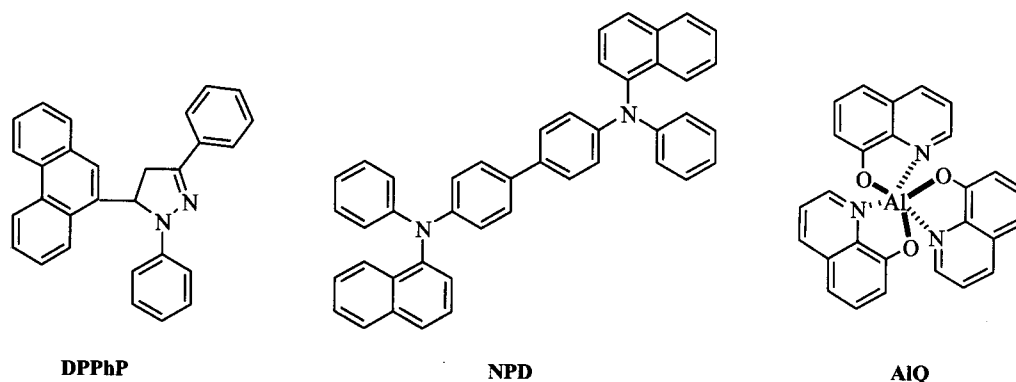


Fig. 1 Molecular structures of DPPhP, α -NPD and AlQ.

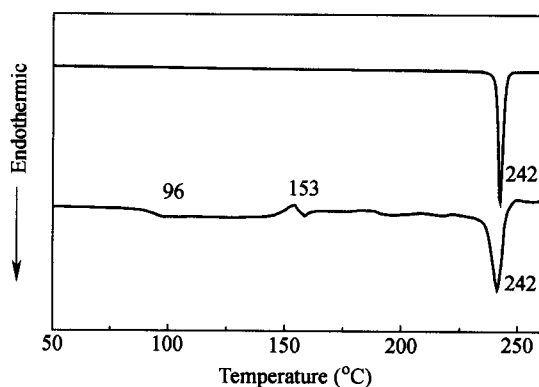


Fig. 2 DSC thermograms of DPPhP (heating rate: 10 °C/min).

heated from room temperature, an endothermic peak due to the melting was observed at 242 °C. When the sample was rapidly cooled down with liquid nitrogen, it changed into an amorphous glassy state. When the amorphous glassy sample was again heated, an endothermic phenomenon was observed at 96 °C, at which the glassy state changed into the super-cooled liquid state. Then a broad exothermic peak due to the crystallization was observed around 153 °C, followed by the endothermic peak due to the melting point at 242 °C. This result shows that DPPhP has a high T_m of 242 °C and a high T_g of 96 °C. The high T_m and T_g promise DPPhP film good thermal stability in EL device. Fig. 3 shows the surface morphology of an evaporated thin film of DPPhP observed from atomic force microscopy (AFM). The thin film was deposited on a cleaned indium tin oxide (ITO) glass substrate by vacuum deposition at 2×10^{-3} Pa. The deposition rate is about 0.3 nm/s and the thickness of the film is about 100 nm. Obviously, the vapor deposited DPPhP

film exhibits an entirely amorphous and flat surface with average roughness (R_a) of about 0.37 nm.

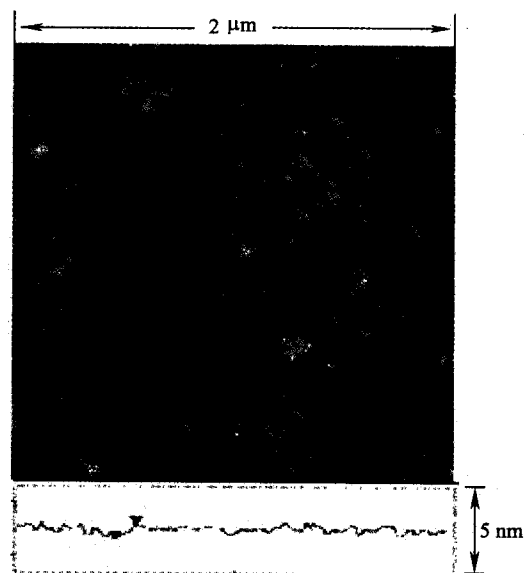


Fig. 3 AFM micrograph revealing the DPPhP film surface morphology.

Cyclic voltammetry (CV) was used to study the redox properties of DPPhP and to estimate the HOMO and LUMO levels. The onset oxidation potential of DPPhP was found to be 0.53 V at the Pt electrode vs. SCE in $\text{CH}_3\text{CN-Bu}_4\text{NBF}_4$ (0.1 mol/L), while the value of α -NPD was found to be 0.78 V under the same conditions. According to the calculation by Noyes,¹³ NHE is taken to be -4.5 eV vs. vacuum. This leads to a potential of -4.74 eV vs. vacuum for SCE. Consequently, the HOMO level was calculated as $\text{HOMO} = -(E_0^{\text{OX}} + 4.74)$ eV. Based on this equation, the HOMO energies of DPPhP and α -NPD were calculated to be -5.27 eV and

-5.52 eV, respectively. The energy levels of electrodes and organic materials are shown in Fig. 4. It is noted that the work function of ITO is -5.4 eV due to oxygen plasma treatment.¹⁴ From the low oxidation potential of DPPhP it can be inferred that hole injection from ITO to DPPhP should be even more efficient than to α -NPD. Additionally, a rather important hole injection barrier of 0.43 eV is expected at the interface between DPPhP and AIQ. In view of the good film forming ability, high T_g and barrierless hole injection from the ITO anode, DPPhP is a very promising hole-transport material. As demonstrated below, it behaves similarly or even better than α -NPD in OLEDs.

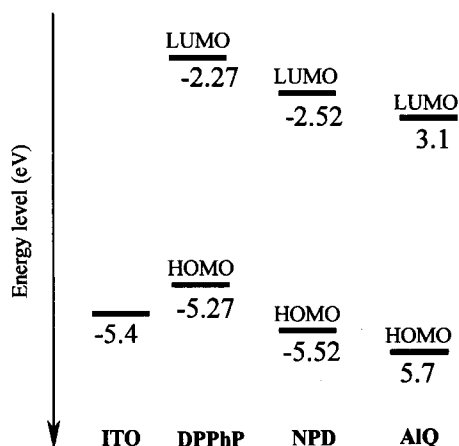


Fig. 4 Energy levels of electrodes and organic materials.

To study the EL performance of DPPhP, a double layer diode structure composed of ITO/DPPhP (60 nm)/AIQ (60 nm)/LiF (0.8 nm)/Al (device A) was fabricated and compared to a reference device using α -NPD instead of DPPhP as hole-transport layer (device B). When the diodes were driven in forward bias, both devices emitted similar green light with peak at around 540 nm, which is attributed to the emission of AIQ.¹ This suggests that DPPhP served as hole-transport layer in device A, similarly to α -NPD in device B.

Fig. 5 gives the current density-voltage ($J-V$) and brightness-current density ($L-J$) characteristics of the two EL devices. It appears that the current density is lower for device A, but its light output at a given current density is higher than for device B. Fig. 6 provides plots of the external quantum efficiency versus driving voltage for both devices. From this figure, it is found that device A using DPPhP as hole-transport layer shows

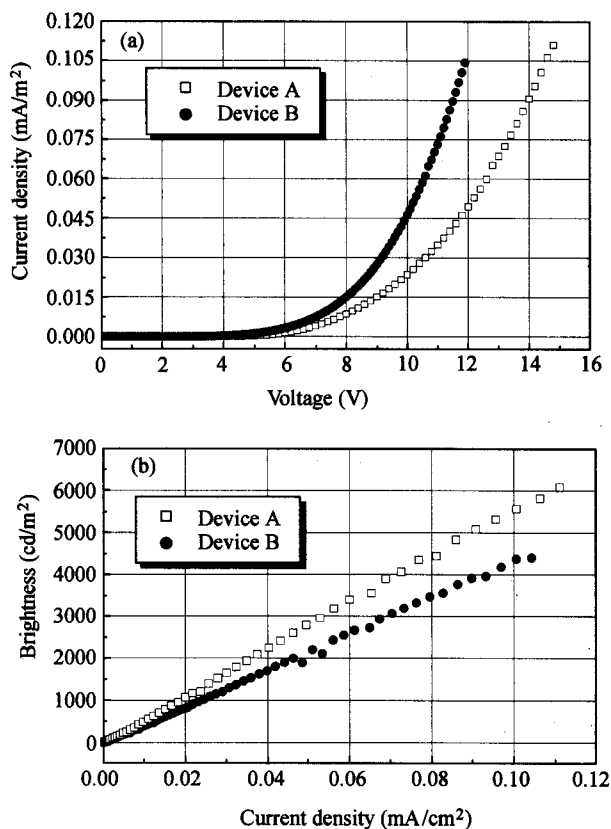


Fig. 5 $J-V$ (a) and $L-J$ (b) characteristics for devices A and B.

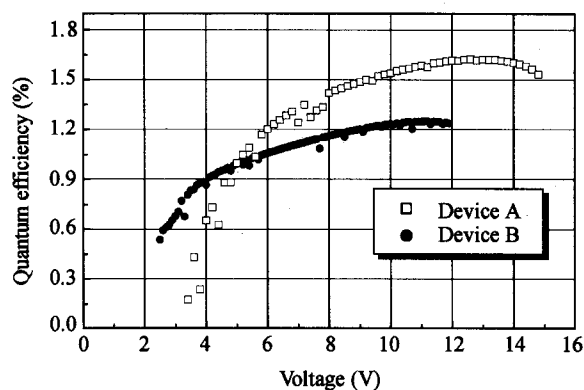


Fig. 6 External quantum efficiency as a function of bias voltage for devices A and B.

higher efficiency than device B. The maximum external quantum efficiency of device A is 1.6% (5.5 cd/A, 60 mA/cm², 3402 cd/m², 12.6 V), while 1.2% (4.4 cd/A, 79 mA/cm², 3475 cd/m², 11.2 V) for device B. The performance at a current density of 20 mA/cm² is summarized in Table 1 for both devices. Clearly, device

Table 1 Device performances of devices A and B at 20 mA/cm².

Device	HTM	λ_{em} (nm)	L (cd/m ²)	External efficiency (%)	Power efficiency (lm/W)
A	DPPhP	541	1066	1.52	1.71
B	α -NPD	531	828	1.15	1.46

A shows a 30% higher efficiency and brightness as compared to device B. The high efficiency of devices using **DPPhP** as HTM was attributed to a better hole confinement and more efficient recombination at the **DPPhP/AIQ** interface. The rather high energy barrier for holes at this interface could as well be responsible for the lower current densities observed in device A.

In summary, we have explored a novel hole-transport material, **DPPhP**, which possesses good film forming ability, high HOMO energy level, and shows excellent hole-transport property in OLEDs. The EL device with structure **ITO/DPPhP/AIQ/LiF/Al** using **DPPhP** as hole-transport layer showed an external efficiency as high as 1.6%.

References and notes

- 1 Tang, C. W.; VanSlyke, S. A. *Appl. Phys. Lett.* **1987**, *51*, 913.
- 2 Ikai, M.; Tokito, S.; Sakamoto, Y.; Suzuki, T.; Taga, Y. *Appl. Phys. Lett.* **2001**, *79*, 156.
- 3 Tang, C. W.; VanSlyke, S. A.; Chen, C. H. *J. Appl. Phys.* **1989**, *65*, 3610.
- 4 Shen, Z.; Burrows, P. E.; Bulović, V.; Forrest, S. R.; Thompson, M. E. *Science* **1997**, *276*, 2009.
- 5 VanSlyke, S. A.; Chen, C. H.; Tang, C. W. *Appl. Phys. Lett.* **1996**, *69*, 2160.
- 6 (a) Thelakkat M.; Schmidt, H. W. *Adv. Mater.* **1998**, *10*, 219.
(b) Katsuma K.; Shirota, Y. *Adv. Mater.* **1998**, *10*, 223.
- 7 Salbeck, J.; Weissortel, F. *Macromol. Symp.* **1997**, *125*, 121.
- 8 Koene, B. E.; Loy, D. E.; Thompson, M. E. *Chem. Mater.* **1998**, *10*, 2235.
- 9 Chen, C. H.; Shi, J.; Tang, C. W. *Macromol. Symp.* **1997**, *125*, 1.
- 10 Sano, T.; Fujii, T.; Nishio, Y.; Hamada, F.; Shibata, K.; Kuroki, K. *Jpn. J. Appl. Phys., Part 1* **1995**, *34*, 3124.
- 11 Donald, E. R.; Judi, R.; John, F. K. W. *Aust. J. Chem.* **1979**, *32*, 1601.
- 12 M.p.: 245–247 °C; $T_g = 96$ °C; ¹H NMR (CDCl₃, 400 MHz) δ : 3.14–3.23 (m, 1H), 4.06–4.17 (q, $J = 13.3, 15.7$ Hz, 1H), 5.95–5.99 (m, 1H), 6.8 (t, $J = 6.9$ Hz, 1H), 7.12–7.21 (m, 5H), 7.32 (d, $J = 7.2$ Hz, 1H), 7.38 (t, $J = 7.6$ Hz, 2H), 7.54 (t, $J = 7.5$ Hz, 1H), 7.63 (t, $J = 7.1$ Hz, 1H), 7.65–7.76 (m, 5H), 8.15–8.17 (m, 1H), 8.67 (d, $J = 7.2$ Hz, 1H), 8.82–8.85 (m, 1H); IR (KBr) ν : 3050, 3025, 2898, 1597, 1505, 1490, 1399, 1338, 1143, 1051, 752, 724, 688 cm⁻¹; MS m/z (%): 398 (M⁺, 33.68), 306 (21.97), 221 (30.13), 91 (100). Anal. calcd for C₂₉H₂₂N₂: C 87.41, H 5.56, N 7.03; found C 87.37, H 5.62, N 7.05.
- 13 Noyes, R. M. *J. Am. Chem. Soc.* **1962**, *39*, 309.
- 14 Nüesch, F.; Carrara, M.; Schaer, M.; Romero, D. B.; Zuppiroli, L. *Chem. Phys. Lett.* **2001**, *347*, 311.